Field Assisted Sintering Technique/Spark Plasma Sintering (FAST/SPS) as a promising method for upcycling of waste materials

Martin Bram (Forschungszentrum Jülich GmbH, 52425 Jülich, Germany) m.bram@fz-juelich.de, Sebastian Jäger (Bergische Universität Wuppertal, 42651 Solingen, Germany) jaeger.fuw@uni-wuppertal.de, Tarini Prasad Mishra (Forschungszentrum Jülich GmbH, 52425 Jülich, Germany) t.mishra@fz-juelich.de, Arne Röttger (Bergische Universität Wuppertal, 42651 Solingen, Germany) roettger@uni-wuppertal.de, Sebastian Weber (Ruhr-Universität Bochum, 44801 Bochum, Germany) weber@wtech.rub.de.

Abstract
During the machining of metals and alloys, a lot of waste is generated, which is expected to become a critical issue under ecological and economical aspects in future. In the present work, an upcycling strategy is introduced on the example of grinding swarf, which can be effectively implemented in a circular economy. For demonstration, grinding swarf of a X155CrVMo12-1 steel (DIN EN 1.2379 / AISI D2) was cleaned, characterized and separated into powder fractions. Afterward, field-assisted sintering technique/spark plasma sintering (FAST/SPS) experiments using conventional graphite tools were conducted to consolidate the swarf directly. Temperature and pressure were varied to improve the densification. As a reference, grinding swarf was processed by supersolidus liquid phase sintering (SLPS) and hot isostatic pressing (HIP). The sintered compacts were characterized regarding density, microstructure, phase composition and Vickers hardness. Special attention was paid to the question of how residuals from the grinding process influence the microstructure.

1. Introduction

Innovative recycling strategies and the introduction of an energy-efficient circular economy for critical raw materials are important prerequisites for the success of the "Energiewende". An attractive approach here is the recycling of materials via powder metallurgical technologies. In addition to the crushing of metallic components at the end of the lifecycle with subsequent powder-based shaping, waste from machining of metallic materials can be returned directly back to the material cycle. The advantages of this recycling strategy are obvious. Since the material is recycled itself, a large amount of energy is saved, which would be needed to synthesize the material when starting again from the primary raw materials. Furthermore, waste that is deposited currently in a scale of many thousand tons per year [1-3] can be returned to the material cycle and a currently unused source of critical raw materials such as Co, W or Mo can be developed [4-7]. Although the basic idea of recycling via the powder metallurgy route is simple, the technical implementation is complex. In order to be able to realize a closed material cycle focused on a powder-based recycling strategy, the following challenges must be properly solved. 1) The components or chip waste must be classified with regard to their chemical composition and varietally collected. 2) The crushing of the components or the processing of the chips must be carried out in an energy-efficient manner and with reproducible results. 3) Impurities taken up during the processing of the material must either be reliably separated or suitably integrated into the cycle. In an ideal case, recycling might even lead to improved material properties (so-called upcycling) [8-12]. 4) Powders derived from recycling processes often have unsuitable powder properties for established powder-based technologies like pressing with subsequent sintering. Accordingly, there is a great need to develop sintering methods adapted to the specific characteristics of recycling powders, which also adequately consider the increasingly important aspect of energy efficiency. 5) On a long-term scale, the goal is to introduce a closed material cycle, in which the material design is already adapted to the requirements of a circular economy, aiming to obtain the value of the material in the cycle as long as possible.

The present work focus on investigating the recycling potential of grinding swarf from the metal-working industry. During grinding, an uptake of lubricants and cooling liquid as well as abrasive particles from the grinding wheel takes place. While for the separation of the liquid components already successful recycling concepts exist [13], abrasive particles usually cannot be removed completely even when applying a magnetic separation process. Many abrasive materials used in grinding processes, such as Alumina, are not soluble in the metallic matrix and cause that recycling of grinding swarf is not worthwhile according to today's processing standards. Nevertheless, we see a potential for recycling grinding swarf via powder metallurgy when a material cycle is developed, allowing the direct shaping of the grinding swarf after purification from the impurities introduced during processing. A further added value is achieved when the residual grinding particles either become alloying elements e.g. by solving them in the bulk or when they take a function in the recycled material e.g. to increase the wear resistance. In the present work, this concept was introduced using grinding swarf from industrial knife production as starting material. Therefore, the grinding swarf consisting of

X155CrVMo12-1 steel (DIN EN 1.2379 / AISI D2) was characterized with respect to particle size distribution and morphology, subsequently prepared and then directly compacted by field assisted sintering technology/spark plasma sintering (FAST/SPS). As a benchmark, the same swarf was densified by supersolidus liquid phase sintering (SLPS) [14,15] and hot isostatic pressing (HIP). The sintered samples were characterized regarding their density, microstructure, phase composition and Vickers hardness. Possible applications of the recycled swarf material are tools for metal-working industry, indexable inserts, or wear-resistant valve coatings, but due to the early stage of development, the final application of the recycled material is not in the focus of the present study.

2. Experimental

2.1 Preparation of grinding swarf

X155CrVMo12-1 (DIN EN 1.2379 / AISI D2) steel is well-established material for industrial knives. The steel belongs to the group of ledeburitic cold-work tool steels and is classified as a high-alloy steel [16]. For long-term stable operation, knife materials must combine high hardness and high ductility. To achieve these properties, the steel has to be heat treated before machining to the final shape [17]. Therefore, the bulk material is hardened and tempered three times in the regime of secondary hardness. After this heat treatment, the steel contains M_7C_3 eutectic carbides and smaller secondary carbides, both embedded in a metal matrix consisting of annealed martensite. When grinding this material, micro-chips with particle sizes ranging from a few micrometers up to several millimeters are formed. The grinding process does not change the phase composition, but it is obvious that the carbides support the formation of small micro-chip scaled particle fractions due to originating fracture. Contrary to waste appearing in the case of turning or milling, grinding swarf is contaminated by cooling lubricant from the grinding process, binder material from the grinding wheel, and last but not least abrasive particles from the grinding wheel [13]. In the present study, the grinding wheel contained Al_2O_3 and SiC particles as abrasive phases. Due to the high moisture content, the grinding sludge was dried at first. Drying was conducted in a drying chamber equipped with an electrical heater. The temperature of the chamber was 150°C, the dwell time was 48 h. During drying, the grinding sludge was continuously rotated for homogeneous removal of moisture. After drying, the swarf was separated into seven particle fractions in a sieve tower by using sieves with varying mesh sizes (1000 µm, 500 µm, 250 µm, 125 µm, 63 µm, and 45 µm). Then, contamination with abrasive particles was clearly reduced by a magnetic separation process. Therefore, the ferromagnetic swarf was attracted by a permanent magnet placed above the swarf, while the anti-ferromagnetic abrasive particles remained on the support. Then, the swarf was removed from the magnet by a non-magnetic scraper. The magnetic separation process was repeated four times. In this preliminary study, only the particle fraction <45 µm was used for subsequent investigations. Energy-dispersive X-ray spectroscopy (EDS) surface scans showed an abrasive particle content in the screen fraction used of less than 3 wt. %. The value demonstrates the effectiveness of the magnetic separation, since the content before this treatment was approx. 20 wt. %.

2.2 FAST/SPS

For FAST/SPS densification, HP-D 5 device from FCT Systeme GmbH (Rauenstein, Germany) and graphite tools with a diameter of 20 mm were applied. Fine-grained SIGRAFINE R7710 graphite (SGL Carbon GmbH, Germany) was used as tool material for cycles with 50 MPa pressure. Isostatically pressed graphite grade 2334 from Mersen, France, was used for cycles at 120 MPa. A graphite foil (SIGRAFEX, SGL Carbon GmbH) with a thickness of 0.35 mm was inserted in the tool before filling to improve the contact between the tool and the swarf. In each sintering cycle, approximately 5 g swarf was poured into the die. After sintering, the height of the samples was around 5 mm. **Table 1** summarizes all FAST/SPS parameters used in this study. Maximum temperature was varied between 950°C and 1150°C. At 1050°C, the pressure was varied to 50 and 120 MPa. Heating rate of 100 K/min and dwell time of 5 min were kept constant for all samples. The atmosphere in the FAST/SPS chamber was Argon.

Table 1: Overview of FAST/SPS parameters used in this study.

Sample ID	Temperature [°C]	Pressure [MPa]
FAST/SPS 1	950	50
FAST/SPS 2	1050	50
FAST/SPS 3	1050	120
FAST/SPS 4	1080	50
FAST/SPS 5	1100	50
FAST/SPS 6	1150	50

2.3 Processing of reference samples by SLPS and HIP

Reference samples were produced by SLPS and HIP using the swarf fraction <45 µm. For more details, we refer to recent publications [14,15]. In SLPS, a temporary liquid phase appears, which

forms a network around the solid phase and supports the densification by viscous flow and capillary forces. Based on thermodynamic calculations, SLPS parameters were adjusted to achieve a liquid phase amount in the range of 20 – 40 vol. %. HIP was conducted in evacuated steel cans. **Table 2** summarizes the processing parameters of both methods.

Table 2: SLPS and HIP processing parameters used for the processing of the reference samples.

Sample ID	Heating rate [°C/min]	Temperature [°C]	Pressure [MPa]	Dwell time [min]	Atmosphere
SLPS	15	1300°C	pressureless	60	Vacuum (5 Pa)
HIP	15	1050	150	240	Inert gas

2.4 Characterization methods

The particle size was measured by sieve analysis using a sieve tower and sieves with varying mesh sizes, as mentioned before using the screening tower AS200 from Retsch. The density of the sintered samples was measured by the Archimedes principle (Measurement of buoyancy by precision balance of type ABJ 220-4NM from Kern & Sohn GmbH) and by image analysis with the reflected-light microscope from Leica of type 6000D. The microstructures were analyzed by SEM (Type Vega 3 SBH from Tescan) equipped with EDS (XFlash 5030 by Bruker). Chemical composition of the grinding swarf was measured by optical emission spectroscopy (Thermo ARL 3460 B). Melting temperature and carbide content of the grinding swarf were calculated using the software Thermocalc with the TCFe9 database. Hardness of the sintered samples was analyzed by Vickers indents (HV0.5) using the Carat 930 by ATM.

3. Results and discussion

3.1. Characterization of grinding chips

A specific characteristic of grinding processes is that the abrasive particles have different morphologies, sizes and geometrically undefined cutting edges, which are simultaneously active [18]. As consequence, the degree of shredding of the starting material into microchips depends on the specific interaction of the material with the respective cutting edge. Therefore, a broad particle size distribution of the grinding swarf results [19]. Sieving is an effective method to separate and fractionize the grinding swarf and to reduce the amount of abrasive particles. **Figure 1** shows the related particle size distribution, which contains a distinct amount of particles larger than 500 µm. 15% of the fragments are even in the millimeter range. The particle size of the residual abrasive particles is mainly in the range of 125 – 500 µm. Due to their irregular and elongated shape (**Figure 2**), swarf particles tend to form agglomerates by interlocking of smaller particles. Therefore, particles larger than 500 µm are mainly agglomerates. As a side effect of interlocking, inclusion of abrasive particles might happen to aggravate their removal by magnetic separation. To increase the amount of finer particles, which is expected to be advantageous with respect to subsequent powder metallurgical processing, milling is an attractive option. Preliminary tests showed the potential (results not shown here), but more systematic studies are required to achieve reproducible results and draw sound conclusions.

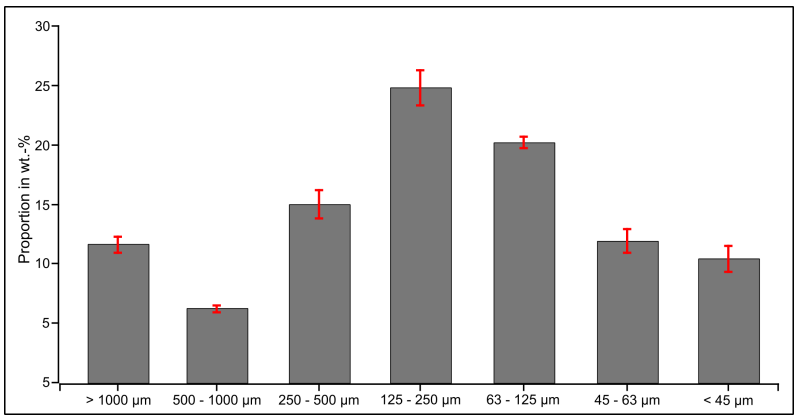

Figure 1: Particle size distribution of dried grinding swarf after separation in a sieve tower.

Figure 2 shows the morphology and microstructure of the grinding swarf on the example of the fraction < 45 µm. At lower magnification, residual abrasive particles are clearly visible as bright phase (**Figure 2a**). At higher magnification, it becomes obvious that the particles still contain carbides of type M_7C_3 as well as Cr-rich secondary carbides close to the stoichiometry of $M_{23}C_6$, which originate from the primary heat treatment of the knife material. The carbides are embedded in a martensitic matrix.

Conventional powder metallurgical processing is limited by the low apparent density and tap density. The fraction <45 µm, which was used in this work, had an apparent density of 0.79 ± 0.02 g/cm³ and a tap density of 1.01 ± 0.03 g/cm³. This leads to a Hausner-factor of 1.33. It was not possible to measure a flowability of the swarf.

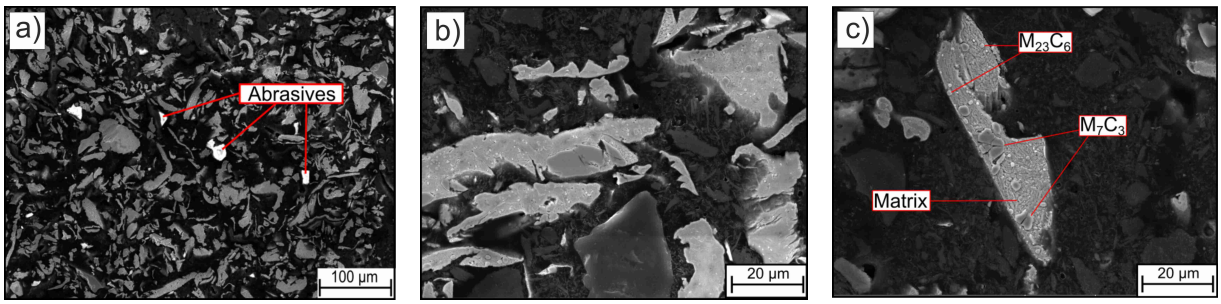

Figure 2. Morphology and microstructure of the grinding swarf fraction < 45 µm. **a)** Residual abrasive particles are visible as bright phase **b,c)** Coarse M_7C_3 and fine Cr-rich secondary carbides are embedded in a martensitic matrix.

Table 3 compares the chemical composition of the grinding swarf (fraction <45 µm) with the nominal composition of the knife steel as defined in DIN EN 1.2379 / AISI D2.

Table 3: Chemical composition of grinding swarf measured by EDS and nominal composition. All values in wt. %.

	Fe	C	Si	Mn	Cr	Mo	V
Nominal composition	bal.	1.55	0.40	0.30	11.80	0.75	0.82
Grinding swarf (EDS + combustion analysis)	bal.	2.61	0.71	0.21	10.45	0.78	0.75

Table 3 shows that the contents of carbon and silicon are beyond the nominal composition of X155CrVMo12-1 steel. The increased carbon content was confirmed by combustion analysis. Here, a content of 2.61 ± 0.20 wt. % was measured. The significant increase of Si and C hint on uptake of SiC residues in the bulk material. The change of chemical composition is coupled with a change in the melting behavior of the grinding swarf. Thermodynamic calculations were done to estimate the shift of the melting temperature compared to the nominal composition of the steel (**Figure 3**). Calculations predict a clear shift of the solidus temperature to lower values, and carbon residues are mainly responsible for this. This strong dependence of the melting behavior from the carbon content must be taken carefully into consideration when conducting FAST/SPS cycles with the material in graphite tools. The direct contact between steel and graphite at elevated temperatures might further increase the carbon content in the bulk shifting the liquid phase formation to even lower temperatures.

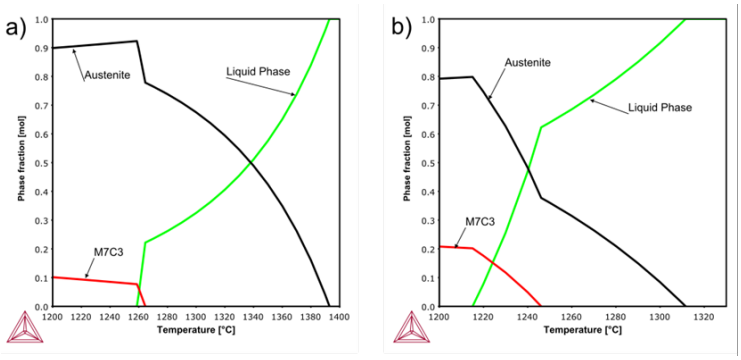

Figure 3: Thermodynamic calculation of the phase composition depending on the sintering temperature for **a)** the nominal composition of the primary material (X155CrVMo12-1) and **b)** the chemical composition of the grinding swarf measured by EDS and combustion analysis.

3.2. Densification of grinding chips by FAST/SPS, SLPS and HIP

The sintering density depends strongly on the processing parameters. **Table 4** summarizes the densities and hardness of the six FAST/SPS samples. Furthermore related values for SLPS and HIP samples are given as a benchmark. In the case of FAST/SPS, maximum densification was achieved at 1050 °C and 120 MPa, as confirmed by both kinds of density measurements. With a further increase of temperature, the sample density decreased and the porosity of the samples increased. At temperatures above 1050°C, partial or complete melting of the sample occurred probably due to

exceeding the solidus temperature, especially at the contact areas between graphite tools and the grinding swarf.

Table 4: Overview of sample densities and hardness values for all samples considered in this study.

Sample-ID	Density Archimedes [% th.d.]	Density image analysis [% th.d.]	Vickers hardness [HV 0.5]	Remarks
FAST/SPS_1	89.5	87.4	579 ± 44	
FAST/SPS_2	89.8	86.8	601 ± 34	
FAST/SPS_3	90.6	88.8	626 ± 73	
FAST/SPS_4	89.7	87.6	584 ± 47	Sample sticks on graphite tool
FAST/SPS_5	n.m.	82.6	556 ± 61	Sample partly molten
FAST/SPS_6	n.m.	69.4	540 ± 52	Sample molten
SLPS	89.7	86.02	602 ± 10.3	
HIP	n.m.	91.63	726 ± 13.9	

n.m. = not measured

The microstructure analysis of selected samples (**Figure 4**) confirms the clearly reduced amount of residual pores in FAST/SPS samples sintered at 1050°C and HIP samples sintered at the same temperature. In the case of SLPS, even at a temperature of 1300°C with large amount of liquid phase formation, lower densification was achieved. In all cases, residual abrasive Al_2O_3 particles were visible within the microstructure (marked by red arrows). EDS revealed their Al_2O_3-type. Contrarily, SiC-type abrasives were not detectable as distinct phases anymore. This suggests that abrasive particles of SiC-type were completely dissolved in the bulk material changing its chemical composition. This effect has been observed for all processing methods considered in this study.

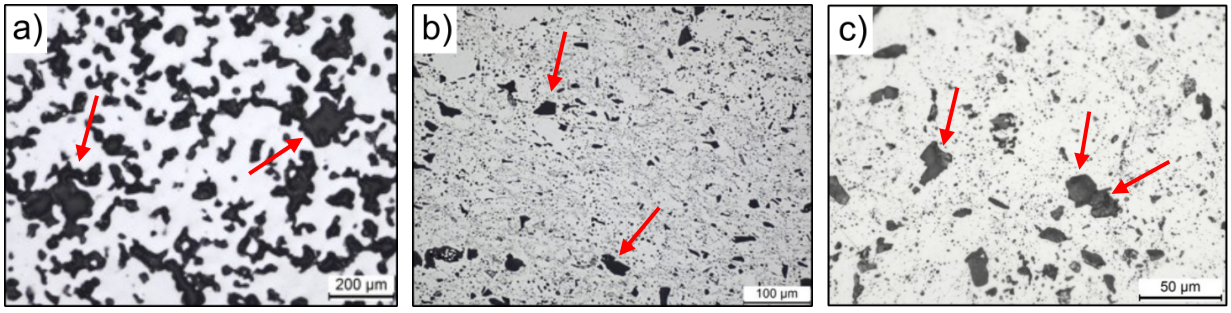

Figure 4: Microstructures of a) SLPS sample b) HIP sample and c) FAST/SPS_3 sample. Abrasive Al_2O_3 particles are marked by arrows.

As a further characterization method, hardness measurements of the different samples were conducted. FAST/SPS samples processed with optimized parameters achieved hardness values of 626 ± 73 HV 0.5. Remarkable scattering of the hardness is caused by the presence of abrasive particles and residual pores. In the case of partial melting of FAST/SPS samples, hardness dropped down to 540 ± 52 HV 0.5. On the other hand, the hardness measurements of the SLPS and HIP samples were 602 ± 10.3 and 726 ± 13.9 in the initial state. Due to the specific processing conditions in HIP with rapid cooling, hardness was significantly increased compared to FAST/SPS and SLPS samples. A comparison between FAST/SPS and SLPS specimens – both in a non-heat treated condition – led to comparable values.

4. Conclusions

In the present study, the potential of FAST/SPS for the recycling of grinding swarf from industrial knife production was investigated. The swarf consisted of a X155CrVMo12-1 steel and the fraction <45 µm was used for the sintering study. Our preliminary results reveal that characteristic FAST/SPS conditions (superposition of direct Joule heating and uniaxial pressure) enable to densify grinding swarf with a particle morphology far from being optimum for conventional powder compaction. Reinforcement of the bulk material by insoluble abrasive Al_2O_3 particles, which were introduced during the grinding process, recommend the recycled material for applications dealing with high wear resistance. After optimization of FAST/SPS parameters, maximum densities of around 90 % were achieved so far. It is expected that an additional milling step might further diminish the agglomerated particles in the grinding swarf increasing the amount of particles, which can be directly compacted by FAST/SPS. This might further reduce the residual porosity. Nevertheless, even in this early stage of development, FAST/SPS implies the following advantages compared to densification by SLPS and HIP.

1) With respect to sintering, the specific kind of FAST/SPS heating enables to increase the heating rate and to lower the required temperature and dwell time, which makes FAST/SPS more effective regarding the cycle time than the other two methods. Compared to HIP, the heating rate was increased by a factor of 6 and the dwell time was reduced by a factor of around 50, while temperature and pressure were kept in the same range. In comparison to SLPS, the sintering temperature was decreased by 200 – 250°C and the avoidance of large amounts of liquid phase makes the FAST/SPS process better controllable. In general, reduction of temperature and dwell time promises a reduction of energy consumption compared to other sintering processes, but careful measurement of energy consumption per part must be done to come to a reliable conclusion. In this context, optimized tool design is one of the key aspects for minimizing energy losses caused by heating of the tool material, heat radiation and water cooling of the electrodes.

2) With respect to shaping, FAST/SPS mainly uses graphite tools, which are easier to manufacture than HIP capsules. When using a special kind of graphite qualities, pressures up to 200 MPa are achievable. Alternative tool materials like Mo-based TZM might enable even higher pressures and longer service life, but restrictions regarding the maximum temperature must be taken carefully into consideration. Compared to HIP, preparing the part for the sintering cycle and removing of the part from the die after the cycle are less laborious. Furthermore, FAST/SPS enables to manufacture semi-finished parts with high dimensional accuracy. When applying multi-component tools, hundreds of parts can be manufactured in one FAST/SPS cycle making this technology competitive to HIP with its possibility of mass production in moderate scale. Today, largest FAST/SPS devices enable to manufacture parts with a diameter beyond 400 mm, but there are process-related restrictions of the height/diameter ratio. For FAST/SPS, different approaches are discussed in literature to manufacture even more complex parts, which can be in principle adapted for the recycling of grinding swarf [20,21]. In contrast to conventional pressing and sintering, near-net-shape production via SLPS technique is more difficult because it is applied on a loose powder bed without a well-defined compaction step. In technical applications, SLPS technology is frequently used for sinter cladding to deposit wear-resistant layers on already contoured parts.

Acknowledgements
The present work is part of the European Regional Development project EffProSchliffUp (EFRE-0801163). The authors highly acknowledge European Regional Development, Leitmarktagentur NRW and ETN (Funding reference number: EU-2-1-005B) for financial and organizational support.

References
[1] E. Erich et al., Bericht AiF-FV-Nr.: 11902 N, 2000.
[2] H.-W. Hoffmeister, et al., Jahrbuch Schleifen, Honen, Läppen und Polieren. (2020) ISBN: 978-3-8027-3133-4.
[3] J. Eckebrecht et al., Härterei-technische-Mitteilung 56 (2001) 126–133.
[4] G. A. Blengini, et al., Resources Policy 53 (2017) 12-19.
[5] E. Brinksmeier, et al., Annals of the CIRP 43 (1994) 593-597.
[6] E. Brinksmeier, et al., J. Mat. Proc. Techn. 44 (1994) 171–178.
[7] A. Schulz, et al., Proc. of United Thermal Spray Conference (1999) 111-116.
[8] H. Eifert, et al., Umwelttechnik 50 (1996) 388-390.
[9] E. Brinksmeier, et al., Zeitschrift für wirtschaftlichen Fabrikbetrieb ZWF 100 (2005) 397-400.
[10] S. Cacace, et al., J. Cleaner Production 268 (2020) 122218.
[11] K.K. Rane, et al., J. Sustainable Metallurgy 3 (2017) 251-264.
[12] T. Shimizu, et al., Mat. Sci. Forum 534-536 (2007) 997-1000.
[13] S. Liedtke, et al., Jahrbuch Schleifen, Honen, Läppen und Polieren, 59. Ausgabe, Vulkan-Verlag, ISBN 3-8027-2919-6, 2000, 112-132.
[14] J. Hankel, et al., J. Cleaner Production 263 (2020) 121501.
[15] S. Jäger, S. Weber, Procedia CIRP 90 (2020) 546–551.
[16] H. Berns, W. Theisen, Eisenwerkstoffe: Stahl und Gusseisen, 4th Edition, Springer-Verlag, 2008.
[17] H. Berns, et al., Härterei-technische Mitteilung 40 (1985) 65–72.
[18] F. Klocke, Fertigungsverfahren 2: Zerspanung mit geometrisch unbestimmter Schneide, 6th ed., Springer Vieweg, Berlin, 2018.
[19] P.-L. Tso, S.-H. Wu, J. Mat. Proc. Techn. 95 (1999) 1–7.
[20] T. Voisin, et al., Adv. Eng. Mat. 17 (2015) 1408 – 1413.
[21] C. Manière, et al., Powder Technology 320 (2017) 340–345.